

Serveur Académique Lausannois SERVAL serval.unil.ch

Author Manuscript

Faculty of Biology and Medicine Publication

This paper has been peer-reviewed but does not include the final publisher proof-corrections or journal pagination.

Published in final edited form as:

Title: Free-breathing 3 T magnetic resonance T2-mapping of the heart.

Authors: van Heeswijk RB, Feliciano H, Bongard C, Bonanno G, Coppo S, Lauriers N, Locca D, Schwitter J, Stuber M

Journal: JACC. Cardiovascular imaging

Year: 2012 Dec

Issue: 5

Volume: 12

Pages: 1231-9

DOI: 10.1016/j.jcmg.2012.06.010

In the absence of a copyright statement, users should assume that standard copyright protection applies, unless the article contains an explicit statement to the contrary. In case of doubt, contact the journal publisher to verify the copyright status of an article.

Title

Free-Breathing Magnetic Resonance T₂-mapping of the Heart for Longitudinal Studies at 3T

Authors

Ruud B. van Heeswijk, PhD*†, H el ene Feliciano, MSc*†, C edric Bongard, BSc‡, Gabriele Bonanno, MSc*†, Simone Coppo, MSc*†, Nathalie Lauriers, MSc‡, Didier Locca, MD‡, Juerg Schwitter, MD‡, Matthias Stuber, PhD*†

Affiliations

*Department of Radiology, University Hospital (CHUV) and University (UNIL) of Lausanne, Switzerland, †Center for Biomedical Imaging (CIBM), Lausanne, Switzerland, ‡Cardiology Service, University Hospital of Lausanne (CHUV), Lausanne, Switzerland

Word count: 3996/4000

Brief title (45ch max): T₂-mapping of the Heart for Longitudinal Studies

Key words: T₂-mapping, longitudinal studies, myocardial infarction

2) Structured Abstract

OBJECTIVES To establish an accurate and reproducible T₂-mapping magnetic resonance imaging (MRI) methodology at 3T and to test it in healthy volunteers and patients with myocardial infarct.

BACKGROUND Myocardial edema affects the T₂ relaxation time on MRI. Therefore, T₂-mapping has been established to characterize edema at 1.5T. A 3T implementation designed for longitudinal studies and aimed at guiding and monitoring therapy remains to be implemented, thoroughly characterized, and evaluated *in vivo*.

METHODS A free-breathing navigator-gated radial MRI pulse sequence with adiabatic T₂Prep and an empirical fitting equation for T₂ quantification was optimized using numerical simulations and was validated at 3T in a phantom study. Its reproducibility for myocardial T₂ quantification was then ascertained in healthy volunteers using an external reference phantom with known T₂. In a small cohort of patients with established myocardial infarction, the local T₂ value and extent of the edematous region were determined and compared to conventional T₂-weighted MRI.

RESULTS The *in vivo* T₂ fitting error was reduced to <1%. The volunteer study consistently demonstrated a reproducibility error as low as 2±1% using the external reference phantom and an average myocardial T₂ of 38.5±4.5ms. In the infarction patients, the T₂ in edema was 62.4±9.2ms, while the spread of the edematous region correlated well between T₂-weighted images and T₂ maps (r=0.91).

CONCLUSIONS The new well-characterized 3T methodology enables robust and accurate cardiac T₂-mapping at 3T, while the addition of a reference phantom improves reproducibility. It may be well-suited for longitudinal studies in patients with suspected or established heart disease.

3) Condensed abstract

A novel T₂-mapping magnetic resonance imaging (MRI) methodology designed for longitudinal studies and aimed at guiding and monitoring therapy was implemented at 3T. The methodology was optimized using numerical simulations and validated in phantom experiments. A healthy volunteer study demonstrated an average reproducibility error of 2±1% using an external reference phantom and an average myocardial T₂ of 38.5±4.5ms. In a small cohort of infarction patients, the T₂ in myocardial edema was 62.4±9.2ms. The new methodology thus enables accurate and reproducible cardiac T₂-mapping at 3T and may be well-suited for longitudinal studies in patients with suspected or established heart disease.

4) Abbreviations list

bpm – beats per minute

bSSFP – balanced steady-state free precession

GRE – gradient echo

MRI – magnetic resonance imaging

ROI – region of interest

STEMI – ST-elevated myocardial infarction

T₂prep – T₂ preparation module

TE – echo time

TR – repetition time

FSE – fast spin echo

5) Text

Introduction

The T_2 relaxation time is a physiological tissue property that can be exploited with magnetic resonance imaging (MRI) to generate contrast between healthy and diseased tissues. This contrast is mainly caused by the dependency of the T_2 value on the relative amount of free water(1). Edema is part of the tissue response to acute injury and affects this free water content. Therefore, T_2 changes have been reported in edematous regions in patients with infarction(2), hemorrhage(3), graft rejection(4), or myocarditis(5). In recent years, *qualitative* T_2 -weighted cardiac MRI has therefore gained considerable interest. However, the traditional dark-blood T_2 -weighted fast spin echo (FSE) pulse sequence that is used for this purpose is limited because of its motion sensitivity and subsequent risk for misinterpretation of the images. Simultaneously, a *quantitative* characterization of the tissue is not easily possible and image interpretation remains subjective. Therefore, a more objective, quantitative and motion-insensitive technique is required. In response to this strong need, initial T_2 -prepared variants of balanced steady-state free precession (bSSFP) sequences have been proposed for quantitative T_2 mapping at 1.5T(6). Using such methods, the successful differentiation between edematous and healthy tissue after myocardial infarction has been demonstrated(7), and an improved performance relative to conventional FSE imaging was reported in both patients with edema after myocardial infarction(8) and acute inflammatory cardiomyopathies(9).

The availability of a quantitative, accurate and highly reproducible T_2 -mapping methodology at 3T would be of great importance for the use in longitudinal studies aimed at monitoring and guiding therapy, since a T_2 value measured within a specific target area could act as its own control measurement. However, to our knowledge both the accuracy and reproducibility of T_2 mapping have not been ascertained. For these reasons, we have developed and tested a free-breathing T_2 -mapping technique at 3T that incorporates radial gradient echo (GRE) image acquisition and adiabatic T_2 preparation (T_2 Prep-GRE). Bloch equation simulations were performed to optimize both sequence parameters and the analysis procedure. The resultant MR methodology was then validated *in vitro*. Quantitative results were compared to

those of a gold-standard spin-echo T_2 mapping sequence to determine the accuracy of the T_2 measurements. The reproducibility of the technique was then investigated in healthy volunteers, both in separate scanning sessions and with and without a T_2 reference phantom positioned in the field-of-view. Using this setup, the hypothesis was tested that the use of a reference phantom improves reproducibility of the T_2 mapping. Finally, the thus-optimized and characterized methodology was applied to test the ability to discern healthy from diseased myocardium in patients with established sub-acute myocardial infarction.

Methods

Numerical Simulations

The goal of these simulations was to maximize the amount of signal per unit time while simultaneously establishing optimal fit parameters to increase the accuracy of the T_2 measurement. Therefore, a numerical simulation of the Bloch equations(10) was performed using Matlab(The Mathworks, Natick, MA). Simulation parameters included myocardial relaxation times $T_2=45\text{ms}$ and $T_1=1470\text{ms}$ (11) at 3T, a segmented k-space radial GRE acquisition with a repetition time (TR) of 7.6ms and an echo time (TE) of 2.8ms, a navigator delay of 40ms and incremental T_2 prep durations ($TE_{T_2\text{prep}}$) of 0, 30 and 60ms for T_2 fitting. The average transverse magnetization (M_{xy}) of radial readouts during 27 heartbeats was then considered representative for the resultant M_{xy} for a given T_2 prep duration. To determine the fitting equation that leads to highest accuracy, the magnetization M_{xy} for three $TE_{T_2\text{prep}}$ values was fitted with both a standard exponential decay and an empirical equation:

$$M_{xy}(T_{T_2\text{prep}}) = M_0 \cdot \left[e^{\frac{-T_{T_2\text{prep}}}{T_2}} + \delta \right], \quad (1)$$

where M_0 refers to the longitudinal magnetization at $TE_{T_2\text{prep}}=0$ and δ is an empirical offset that accounts for T_1 -relaxation. Independent variables that were utilized to study the quality and robustness of the fit and to maximize M_{xy} included heart rate, radiofrequency (RF) excitation angle (α), the number of acquired radial profiles in k-space per heartbeat and the number of RR intervals in-between acquisition trains. After having selected the parameter set that

led to a maximum M_{xy} , the range of stability of the T_2 fitting algorithm was determined for both the standard and empirical equation in a T_2 range from 1 to 250ms, which sufficiently covers physiological T_2 values expected at 3T.

Implementation & Imaging Sequence

The T_2 -mapping segmented k-space radial gradient echo imaging sequence (T_2 prep-GRE) was implemented on two 3T MR scanners (Magnetom Trio and Verio, Siemens Healthcare, Erlangen, Germany) with a 32-channel chest coil (Invivo, Gainesville, FL) and with sequence parameters as described above. Since T_2 preparation at high magnetic field strength is susceptible to B_1 inhomogeneity(12), an adiabatic T_2 Prep(13) with user-specified TE_{T_2Prep} preceded the imaging part of the sequence that had a temporal resolution of 97ms and a spatial resolution of $1.25 \times 1.25 \times 5 \text{mm}^3$. For respiratory motion suppression during free breathing, a lung-liver respiratory navigator(14) was utilized. For each T_2 map, the imaging sequence was repeated with three incremental TE_{T_2Prep} (0, 30 and 60ms). After acquisition of the three source images, affine coregistration(15) was applied to increase the accuracy of the T_2 mapping, before the final pixel-by-pixel computation of the T_2 maps was performed using a custom-written Matlab analysis tool in which the optimized Eq. 1 was incorporated.

Phantom Studies

Seventeen phantoms with different T_2 values that consisted of varying concentrations of NiCl_2 and agar(16) together with sodium azide as a antimicrobial preservative were constructed and T_2 maps were generated with the T_2 prep-GRE sequence to assess the performance of the pulse sequence and to validate the results of the simulations. A spin-echo sequence with 8-11 incremental echo times ($TE=4\text{-}500\text{ms}$, $TR=5\text{s}$) was used to define the ‘gold-standard’ T_2 , while an inversion recovery spin-echo sequence with 8-11 inversion times ($TI=14\text{-}3000\text{ms}$, $TR=7\text{s}$) was used to determine the ‘gold-standard’ T_1 . To characterize the accuracy and precision of the T_2 prep-GRE-derived T_2 values using Eq. 1, a linear correlation with the spin-echo ‘gold standard’ T_2 values was performed. To ascertain whether the phantom T_2 values are subject to change as a function of time, the T_2 values of the phantoms were determined monthly up to 6 months after their construction.

Volunteer Studies

Permission from the institutional review board was obtained for all volunteer and patient scans, and written informed consent was obtained from all participants prior to the procedure. In order to characterize the performance of the GRE-T₂prep T₂-mapping methodology for longitudinal studies, 10 volunteers (6 male, age=27±4 years) underwent two separate scanning sessions with an identical protocol. In-between the sessions, the volunteers were extracted from the scanner room. In order to obtain an external reference standard T₂ value in each measurement, a phantom with known T₁ and T₂ values (see Phantom Studies) similar to those of the healthy myocardium(11) was positioned in the field of view. After shimming of the heart based on a local gradient-echo field map(17), T₂ maps were obtained in a short axis view.

To test the hypothesis that the external reference phantom leads to an improved reproducibility of the T₂-mapping protocol, the two scanning sessions were compared as follows: the entire left ventricular (LV) myocardium in the image and a homogeneous and central area of the phantom were manually segmented by two experienced observers (RBvH, CB) and their average T₂ was directly (without the use of the external reference phantom) calculated ($T_{2myo,dir}$ and $T_{2phan,dir}$). Using the ‘true’, known T₂ value of the phantom $T_{2phan,true}$ as determined with the spin-echo sequence described earlier, a corrected myocardial T₂ value $T_{2myo,corr}$ was calculated:

$$T_{2myo,corr} = T_{2myo,dir} \frac{T_{2phan,true}}{T_{2phan,dir}}. \quad (2)$$

The percentage difference between $T_{2myo,dir}$ and $T_{2myo,corr}$ for both scanning sessions as well as the intra- and inter-observer variability were then calculated.

Patient studies

As a next step, the optimized and validated methodology described above was used in 11 patients (9 male, age=50±13 years) in the unique setting of sub-acute phase after percutaneous coronary revascularization of an acute ST-elevation myocardial infarction (STEMI). Short-axis T₂ maps at a mid-ventricular level were acquired in all patients together with *qualitative* breath-hold black-blood T₂-weighted FSE images (TR/TE=2540/70ms, echo train length = 17).

After calculating the T_2 maps in these patients, the myocardium and the reference phantom were manually segmented. The average T_2 values and standard deviations were subsequently determined in both ROIs and were compared to the values obtained in healthy volunteers. The tissue with elevated T_2 values was considered as being the infarcted region. Simultaneously, a more objective and automated selection of the region of elevated T_2 was selected by only including pixel T_2 values that were 3 standard deviations above the average T_2 value of the healthy myocardium. In both the T_2 maps and the T_2 -weighted FSE images, the center of the segmented left ventricle was selected by the user and the radial extent of the infarction was manually determined as the edge of the continuous spread of the automatically detected elevated T_2 values, after which a linear regression of the spread in the two image types was performed. The automatically selected regions of infarct on the T_2 maps were then also related to the location of the luminal narrowing by X-ray angiography, where available.

Statistical analyses

All statistical tests were paired or unpaired (as applicable) two-tailed Student's t -tests, where $p < 0.05$ was considered statistically significant. Correlations between continuous variables were calculated with the Pearson correlation coefficient r . Coefficients of determination R^2 were calculated for all linear regressions through the origin. Intra- and inter-observer variability were calculated by Bland-Altman analysis(18).

Results

Numerical Simulations

Numerical simulations of the Bloch equations for the pulse sequence resulted in maximum signal per unit time for an RF excitation angle of 20° and 21 radial k -space lines per heartbeat. The empirical fitting equation led to the most accurate T_2 determination if the offset δ was set to 0.06 (Fig. 1a). In contrast, when the conventional exponential curve fitting procedure was applied to the simulated magnetization, the T_2 value was always overestimated by $\sim 12\%$ (Fig. 1b). These findings were consistent over a broad range of simulated T_2 values (Fig. 1c). Further numerical simulations suggested a minor heart-rate dependency of the T_2 measurements relative to 60bpm with a 2.2% underestimation at 90bpm and a 1.5% overestimation at 40bpm.

Phantom Studies

An excellent agreement between the T_2 maps generated with conventional FSE and the T_2 prep-GRE method that incorporates the empirical equation was found in the phantom study (Fig. 2). With a correlation $r=0.996$ and a slope of 0.97, it was found that T_2 computation using the proposed T_2 mapping methodology is accurate and precise over a large range of T_2 . When comparing the T_2 values of the phantoms that were measured 6 months apart, no significant change was observed ($p=0.83$) and the maximum difference that was measured in a phantom over time was 1.5ms.

Volunteer Studies

The optimized protocol was successfully applied in all 10 healthy volunteers (Fig. 3). The directly calculated myocardial $T_{2myo,dir}$ varied $4\pm 2\%$ on average between the two scanning sessions, while the corrected myocardial $T_{2myo,corr}$ obtained using the external reference phantom varied significantly less with $2\pm 1\%$ ($p=0.005$) between scanning sessions (Fig. 3C). Averaged over all volunteers, $T_{2myo,dir}$ was 41.2 ± 4.1 ms, while the average $T_{2myo,corr}$ was 38.5 ± 4.5 ms ($p=0.07$).

The intra-observer mean difference for $T_{2myo,corr}$ was -0.04 ms (confidence interval CI: -1.2 to 0.6 ms, $p=0.86$), while the inter-observer mean difference was -0.4 ms (CI: -1.2 to 0.4 ms, $p=0.87$, Fig. 4).

Patient Studies

The T2prep-GRE T₂-mapping protocol was successfully applied and T₂ maps generated in all 11 STEMI patients, while respiratory motion artifacts led to lower-quality T₂-weighted FSE images in 3 of these cases, of which 1 was excluded from further analyses. On the T₂ maps of the remaining cases, a clear demarcation of regions with elevated quantitative T₂ values visually co-registered with the findings on T₂-weighted MRI and X-ray coronary angiography as shown in Table 1 and the example in Fig. 5. The average T₂ over all patients in the healthy remote region was 41.5±3.6ms. This was statistically significantly higher than that in healthy volunteers (38.5±4.5ms; $p=0.04$), although it should be noted that this average included three severe STEMI patients in which the T₂ value of the healthy remote segment was measured higher than 50ms. The average manually determined T₂ value in the infarcted regions was 61.2±10.1ms, while the automatic method resulted in 62.4±9.2ms ($p=0.27$). There was a good overall correlation between the manually and automatically determined T₂ values ($r=0.91$, slope=1.01, $R^2=0.77$). Furthermore, the circumferential location of the signal-enhanced regions by T₂-weighted FSE imaging and increased T₂ values by T₂ mapping visually agreed very well and corresponded with the myocardial segment that was supplied by the vessel that had a stenosis on the corresponding X-ray angiograms (Fig.6).

A linear regression of the radial spread in the T₂-weighted images and T₂ maps, as illustrated in Fig. 7, demonstrated a slight increase of the radial spread in the images obtained with T₂ mapping ($r=0.92$, slope=0.89, $R^2=0.80$).

Discussion

The presented T₂prep-GRE methodology accurately and reproducibly enables T₂ mapping at 3T during free breathing. A series of incremental steps were essential and enabling for the translation from theory to the patient setting.

Numerical Simulations

Both the empirical equation that was established using Bloch equation simulations and the standard exponential decay model led to an equally good fit. However, since the latter does not take T₁ relaxation into account, a consistent ~12% T₂ overestimation was observed, while the use of the empirical equation resulted in a <1% T₂ underestimation only.

Phantom Studies

The phantom experiments confirmed that the use of the optimized 3T methodology resulted in accurate T₂ measurement relative to conventional spin-echo measurements as the gold standard. However, for maximized performance of the technique and definition of δ , the T₁ of the measured tissue has to be known. This raises concern since the T₁ value of the myocardium may be subject to change. It has been reported(19) that the T₁ of healthy and infarcted myocardium may differ by 18%. Such a change in T₁ would result in a 2.8% underestimation of the T₂ value according to our Bloch equation simulations, which seems acceptable given the standard deviation in T₂ measurements of 6-10% in this study. If the phantoms are to be used in longitudinal studies, the T₁ and T₂ values need to be constant over time. To this end, the antimicrobial sodium azide was added, and it was confirmed that no significant changes in T₂ were detected over the course of 6 months.

Volunteer studies

The methodology was further characterized in an *in vivo* healthy volunteer study where its effectiveness and reproducibility were evaluated. Adding the reference phantom allowed for the compensation of drift between scans. The inter- and intra-observer variability of the corrected T₂ values were similar to those reported in related studies(8,20) at 1.5T. While the T₂ values of healthy myocardium were consistent with those reported in literature

(21), the addition of a reference phantom significantly aided in the reduction of the difference in myocardial T_2 values between two scanning sessions. Such T_2 value differences may occur due to slight changes related to B_0 and B_1 inhomogeneity, the relative accuracy of the fitting procedure, coil placement etc. Furthermore, and consistent with prior reports that established T_2 mapping at lower field strength(6,7), only 3 points were used for the mono-exponential two-parameter fit for the T_2 determination in this study. While more points may result in an improved accuracy and robustness of the procedure, this remains to be investigated and has to be carefully balanced versus an increase in scanning time.

Patient Studies

In the small cohort of 11 STEMI patients, the quantitative T_2 values of the edematous regions (defined on conventional T_2 -weighted imaging) showed an increase of approximately 50% relative to their healthy remote counterparts in all cases. This also enabled a robust automated detection of these regions that correlated well with the more subjectively selected user-specified regions of T_2 enhancement. The T_2 of the healthy remote segments in the patients was slightly but significantly higher than that found in healthy volunteers. However, the study was not age-matched and an age-dependent increase in T_2 between the studied cohorts cannot be excluded.

The circumferential location of elevated signal on T_2 -weighted images and X-ray angiograms agreed very well, as did the comparison of the radial spread of the edematous region as determined through T_2 mapping and T_2 -weighted imaging, which was expected since myocardial contrast in both modalities is based on the degree of edema. However, T_2 -weighted imaging only defines presence and extent of elevated T_2 while T_2 -mapping is quantitative and may therefore provide a very important quantitative endpoint for many studies related to cardiovascular disease.

In the 3 severe STEMI cases, the finding that the measured T_2 value of the reference phantom was unchanged relative to the gold standard measurements, improved confidence that unusually high T_2 values (~50 ms) were indeed found in the unaffected, “healthy” remote myocardial tissue. While the use of an external reference phantom was originally designed to improve inter-scan reproducibility, this suggests that it may equally benefit the accuracy of a

single study in patients where the overall T_2 value of the entire myocardium is elevated. Example applications include studies in myocarditis, heart failure or transplant patients.

In conclusion, the methodology presented in this study enables robust and accurate quantitative cardiac T_2 -mapping at 3T, while the addition of a reference phantom improves reproducibility. Therefore, it may be well-suited for longitudinal studies in patients with ischemic heart disease.

6) Acknowledgments

This work was supported by the Centre d'Imagerie BioMédicale (CIBM) of the UNIL, UNIGE, HUG, CHUV, EPFL and the Leenaards and Jeantet Foundations, as well as the Emma Muschamp Foundation.

7) References

1. Friedrich MG. Myocardial edema--a new clinical entity? *Nat Rev Cardiol* 2010;7:292-6.
2. Payne AR, Casey M, McClure J et al. Bright-blood T2-weighted MRI has higher diagnostic accuracy than dark-blood short tau inversion recovery MRI for detection of acute myocardial infarction and for assessment of the ischemic area at risk and myocardial salvage. *Circ Cardiovasc Imaging* 2011;4:210-9.
3. Eitel I, Kubusch K, Strohm O et al. Prognostic value and determinants of a hypointense infarct core in T2-weighted cardiac magnetic resonance in acute reperfused ST-elevation-myocardial infarction. *Circ Cardiovasc Imaging* 2011;4:354-62.
4. Taylor AJ, Vaddadi G, Pfluger H et al. Diagnostic performance of multisequential cardiac magnetic resonance imaging in acute cardiac allograft rejection. *Eur J Heart Fail* 2010;12:45-51.
5. Zagrosek A, Abdel-Aty H, Boye P et al. Cardiac magnetic resonance monitors reversible and irreversible myocardial injury in myocarditis. *JACC Cardiovasc Imaging* 2009;2:131-8.
6. Huang TY, Liu YJ, Stemmer A, Poncelet BP. T2 measurement of the human myocardium using a T2-prepared transient-state TrueFISP sequence. *Magn Reson Med* 2007;57:960-6.
7. Giri S, Chung YC, Merchant A et al. T2 quantification for improved detection of myocardial edema. *J Cardiovasc Magn Reson* 2009;11:56.
8. Verhaert D, Thavendiranathan P, Giri S et al. Direct T2 quantification of myocardial edema in acute ischemic injury. *JACC Cardiovasc Imaging* 2011;4:269-78.
9. Thavendiranathan P, Walls M, Giri S et al. Improved detection of myocardial involvement in acute inflammatory cardiomyopathies using t2 mapping. *Circ Cardiovasc Imaging* 2012;5:102-10.
10. Bloch F. Nuclear Induction. *Phys Rev* 1946;70:460-74.
11. Stanisz GJ, Odobina EE, Pun J et al. T1, T2 relaxation and magnetization transfer in tissue at 3T. *Magn Reson Med* 2005;54:507-12.
12. Greenman RL, Shirosky JE, Mulkern RV, Rofsky NM. Double inversion black-blood fast spin-echo imaging of the human heart: a comparison between 1.5T and 3.0T. *J Magn Reson Imaging* 2003;17:648-55.
13. Nezafat R, Stuber M, Ouwerkerk R, Gharib AM, Desai MY, Pettigrew RI. B1-insensitive T2 preparation for improved coronary magnetic resonance angiography at 3 T. *Magn Reson Med* 2006;55:858-64.
14. Ehman RL, Felmler JP. Adaptive technique for high-definition MR imaging of moving structures. *Radiology* 1989;173:255-63.
15. Giri S, Shah S, Xue H et al. Myocardial T2 mapping with respiratory navigator and automatic nonrigid motion correction. *Magn Reson Med* 2012.
16. Kraft KA, Fatouros PP, Clarke GD, Kishore PR. An MRI phantom material for quantitative relaxometry. *Magn Reson Med* 1987;5:555-62.
17. Schar M, Vonken EJ, Stuber M. Simultaneous B(0)- and B(1)+-map acquisition for fast localized shim, frequency, and RF power determination in the heart at 3 T. *Magn Reson Med* 2010;63:419-26.
18. Bland JM, Altman DG. Statistical methods for assessing agreement between two methods of clinical measurement. *Lancet* 1986;1:307-10.
19. Piechnik SK, Ferreira VM, Dall'Armellina E et al. Shortened Modified Look-Locker Inversion recovery (ShMOLLI) for clinical myocardial T1-mapping at 1.5 and 3 T within a 9 heartbeat breathhold. *J Cardiovasc Magn Reson* 2010;12:69.
20. Thavendiranathan P, Walls M, Giri S et al. Improved detection of myocardial involvement in acute inflammatory cardiomyopathies using T2 mapping. *Circ Cardiovasc Imaging* 2012;5:102-10.
21. Guo H, Au WY, Cheung JS et al. Myocardial T2 quantitation in patients with iron overload at 3 Tesla. *J Magn Reson Imaging* 2009;30:394-400.

8) Figures

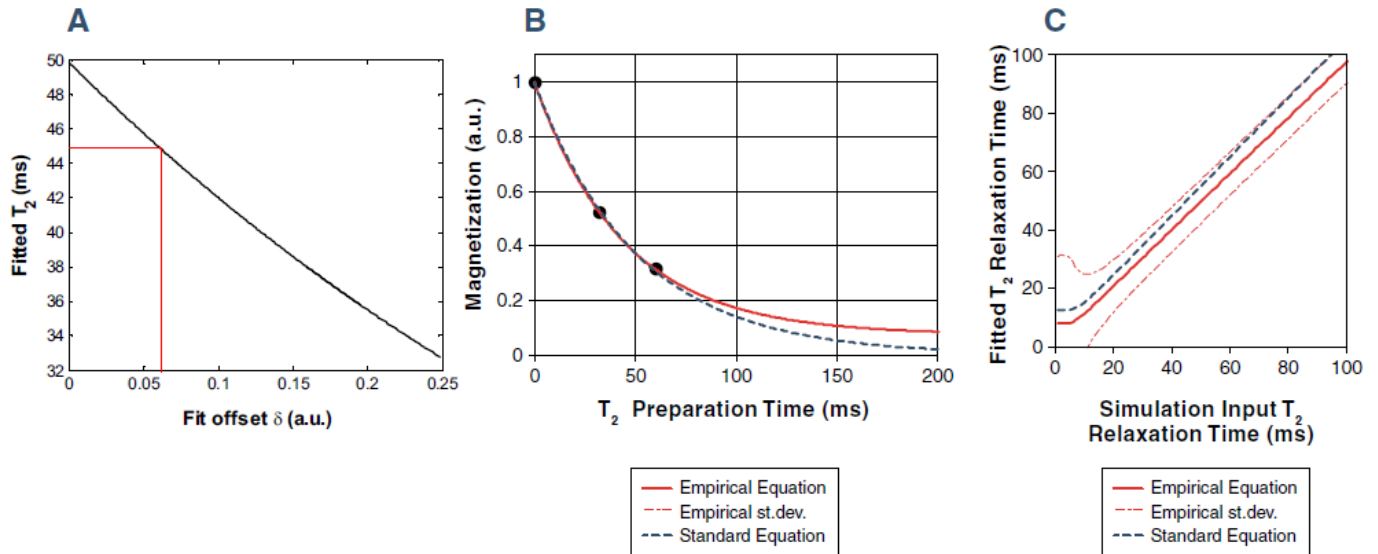


Figure 1. Optimization of T₂-mapping through Bloch equation simulations. (A) The fitted T₂ values as a function of the empirical offset δ and a reference T₂ of 45ms. The red lines indicate the δ that results in a fitted T₂=45ms. (B) Standard (dashed) and empirical (solid, with $\delta=0.06$) curve fits of the magnetization with an input T₂ of 45ms. While both equations fit the simulated magnetization points very well ($R^2=0.99$), the standard equation results in T₂=51±18ms and the empirical equation in T₂=45±17ms. (C) The fitting accuracy of the standard (dashed) and empirical (solid) equations compared to the identity line over a range of T₂ values. While the accuracy of the empirical equation decreases for low T₂ values (<15ms) as evidenced by its increasing standard deviation (dot-dashed), it only slightly underestimated higher T₂ values.

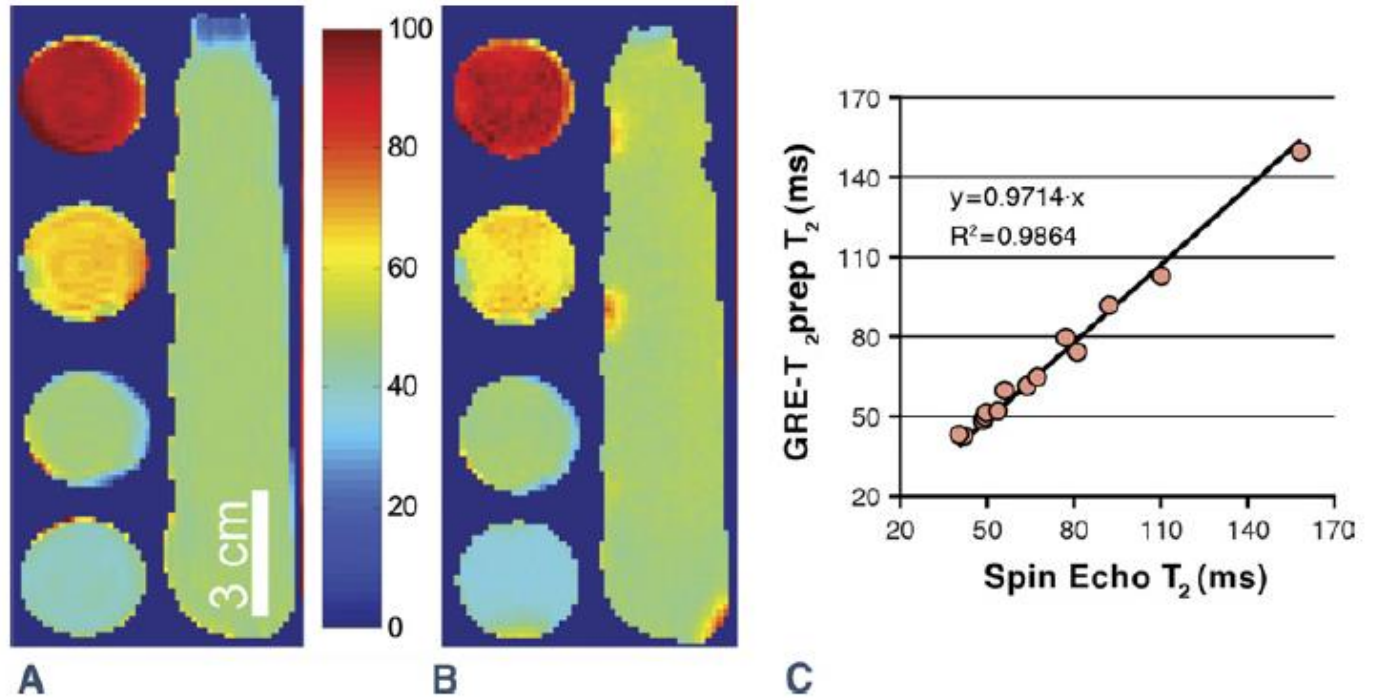


Figure 2. Sequence validation in a series of phantoms. (A) T₂ map of a series of phantoms with different T₂ (four 50ml tubes and a 1L infusion bag), obtained with the spin echo pulse sequence. (B) T₂ map of the same five phantoms obtained with the T₂prep-GRE sequence. (C) Scatter plot of the T₂ values of 15 phantoms obtained with the two T₂-mapping techniques. The linear fit through the origin resulted in a slope of 0.97 (R²=0.99).

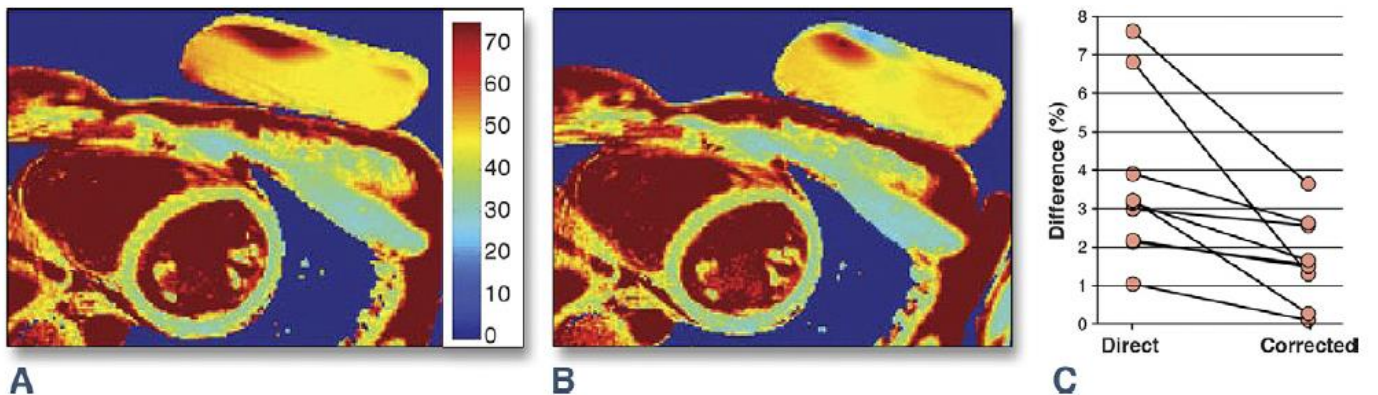


Figure 3. Multiple scan sessions in volunteers. (A) Short-axis T₂ map of the left ventricle of a 26 y.o. female volunteer with a reference phantom on the chest. Only the homogeneous area of the phantom was used for T₂

computations. (B) The same volunteer in the second scanning session. The position of the phantom has slightly changed. (C) Plot of the difference in T_2 values before and after correction obtained in 10 volunteers with the reference phantom (two pairs of lines very narrowly overlap).

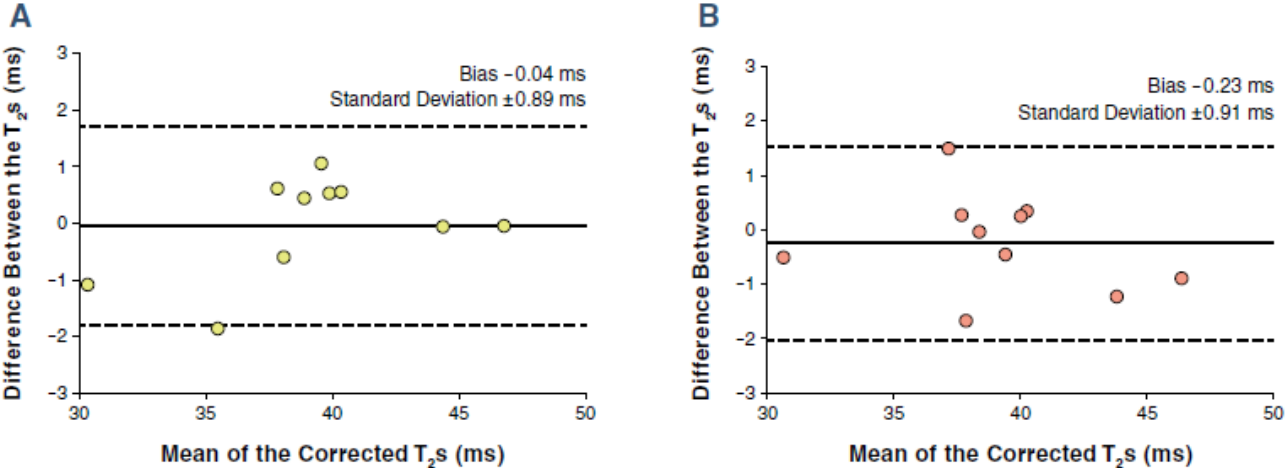


Figure 4. Intra- and inter-observer variability. Bland-Altman plots for the difference between two measurements of a single observer (A) and for the difference between a measurement of two observers (B). The dashed lines indicate the 95%-confidence interval.

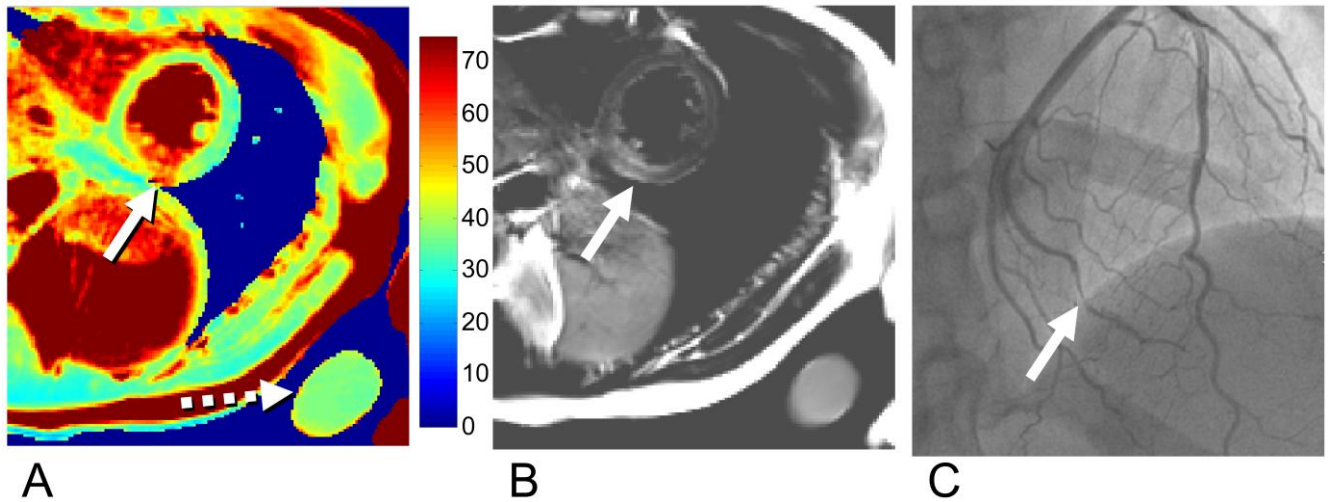


Figure 5. Short-axis T_2 -map together with conventional T_2 -weighted fast spin-echo MRI and an X-ray coronary angiogram in a patient with a small myocardial infarct. (A) A clearly demarcated zone with elevated T_2 can be seen in the region of the black arrow, which might indicate myocardial edema. The non-infarcted tissue has a homogeneous T_2 , while the reference phantom (dotted arrow) appears homogeneous with T_2 values similar to those of healthy tissue. Scaled color bar in ms. (B) The T_2 -weighted FSE image confirms the elevated T_2 in the region of the infarct (arrow). (C) Consistent with these findings, the X-ray coronary angiogram shows a severe stenosis in an obtuse marginal artery (arrow).

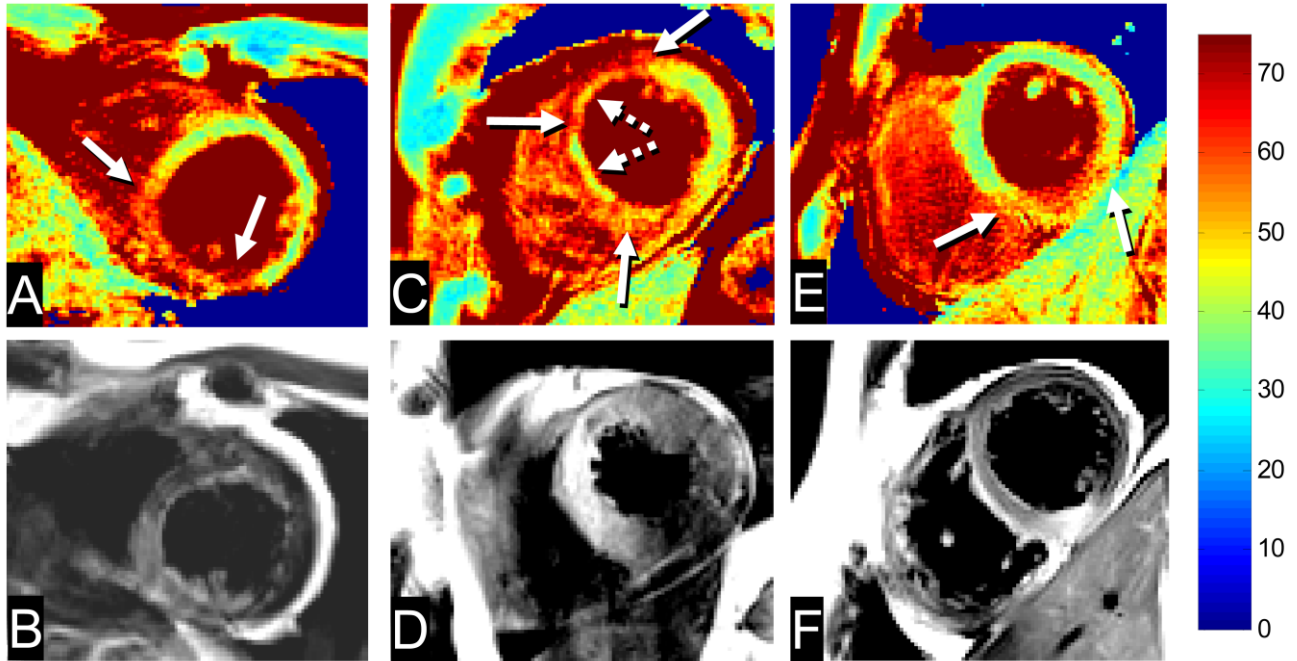


Figure 6. T₂ maps (A,C,E) and conventional T₂ (B,D,F) images of three representative cases. Infarcted regions are indicated with solid arrows on the T₂ maps. Reference phantoms are not shown to provide more detail of the myocardium. (A,B) Posteroseptal STEMI in a 46y.o. man. (C,D) Large septal STEMI in a 72y.o. man. T₂-weighted and T₂-map regions match, but a region of hemorrhage(8) (dashed arrows) can also be discerned in the T₂ map. (E,F) Posterior STEMI in a 38y.o. man.

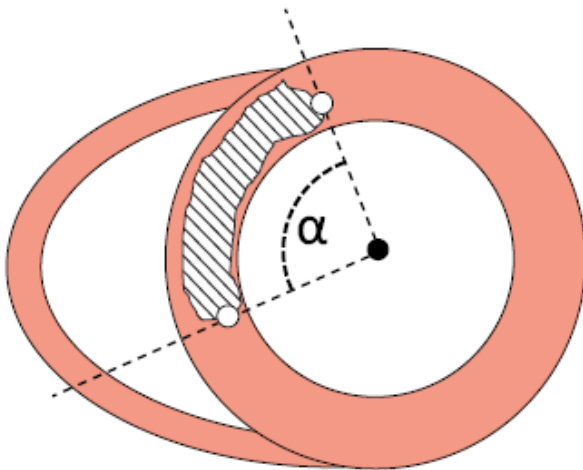
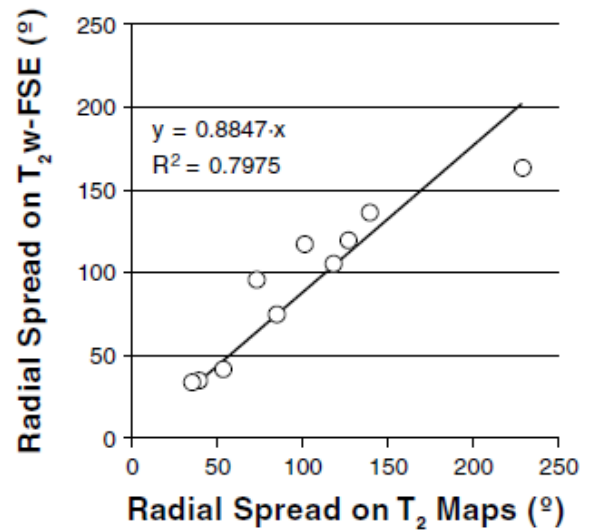
A**B**

Figure 7. Relationship of the angular spread of the infarct as seen on the T₂-weighted images and the T₂ maps. (A) Schematic of the analysis of radial spread of a region of elevated T₂. First, a point is placed in the center of the left ventricle (solid dot). Next, two points are placed on the radial borders of the elevated region (open dots), after which the angle between these points is calculated. (B) Linear regression of the radial spread of the elevated region in T₂-weighted images and T₂ maps in STEMI patients. One patient was excluded since the T₂-weighted image was not of sufficient diagnostic quality.

9) Tables

Table 1. Agreement between X-ray angiography and T₂ mapping. Agreement was said to be found when the T ₂ was elevated in the region that was supplied by the culprit vessel.			
Patient #	X-ray culprit vessel (level of occlusion)	T₂ map affection region	Agreement?
1	Proximal LAD	Anteroseptal	Yes
2	First marginal of LCX	Posterolateral	Yes
3	Proximal RCA	Posteroseptal	Yes
4	Proximal LAD	anterolateral	Yes (border)
5	Proximal LAD	Posteroseptal and anterolateral	Yes (two small zones)
6	Middle RCA	Posteroseptal	Yes
7	Proximal LAD	Posterolateral to anterior	Yes
8	Proximal LAD	Septal	Yes (border)
9	Middle LAD	Posteroseptal	Yes (right dominance)
10	Middle RCA	Posterolateral	Yes
11	Distal RCA	Posterior	Yes

CMR = cardiac magnetic resonance imaging, LAD = left anterior descending coronary artery, LCX= circumflex coronary artery, RCA = right coronary artery